SCIENTIFIC REPⓄRTS

OPEN

Novel nano-semiconductor film layer supported nano-Pd Complex Nanostructured Catalyst Pd/Ⓕ-MeO$_x$/AC for High Efficient Selective Hydrogenation of Phenol to Cyclohexanone

Jiaqi Si, Wenbing Ouyang, Yanji Zhang, Wentao Xu & Jicheng Zhou

Supported metal as a type of heterogeneous catalysts are the most widely used in industrial processes. High dispersion of the metal particles of supported catalyst is a key factor in determining the performance of such catalysts. Here we report a novel catalyst Pd/Ⓕ-MeO$_x$/AC with complex nanostructured, Pd nanoparticles supported on the platelike nano-semiconductor film/activated carbon, prepared by the photocatalytic reduction method, which exhibited high efficient catalytic performance for selective hydrogenation of phenol to cyclohexanone. Conversion of phenol achieved up to more than 99% with a lower mole ratio (0.5%) of active components Pd and phenol within 2 h at 70 °C. The synergistic effect of metal nanoparticles and nano-semiconductors support layer and the greatly increasing of contact interface of nano-metal-semiconductors may be responsible for the high efficiency. This work provides a clear demonstration that complex nanostructured catalysts with nano-metal and nano-semiconductor film layer supported on high specific surface AC can yield enhanced catalytic activity and can afford promising approach for developing new supported catalyst.

Catalytic hydrogenation of phenol to cyclohexanone is a reaction of commercial and environmental significance, for the hydrogenation product is an important raw material for caprolactam and adipic acid, which are the monomer of nylon-6 and nylon-66, respectively[1]. Generally, phenol can be hydrogenation to cyclohexanone in a "one-step" or a "two-step" process. In two-step, phenol is hydrogenated to cyclohexanol firstly and cyclohexanol is dehydrogenated to yield cyclohexanone subsequently[2, 3]. The one-step process avoids the endothermic step of dehydrogenation and therefore is certainly preferable in terms of capital costs and energy savings. Selective directly hydrogenation of phenol to cyclohexanone conducts either in gas or liquid phase in the literatures[4–7]. In general, the vapor phase hydrogenation must experiences harsh conditions such as high pressure and temperature, which usually causes catalyst deactivation by coking, generating undesirable by-products and complicating the separation[8, 9]. Hence liquid phase hydrogenation can be great interest because of the relatively mild reaction conditions[10, 11]. Many researchers have contributed to this area, and multiple catalysts have been screened, such as Pd/C[12], Pd/Al-MCM-41, Ru/Al-MCM-41[13], Pd/MHSS, PdAu/MSHH[14, 15], Pd/MIL-101[16]. However, achieving a high selectivity (95%) at elevated conversion (80%) under mild conditions is a great challenge. Notably, Han and his co-worker[17] reported that a complete phenol conversion with >99.9% selectivity to cyclohexanone could be achieved on a dual-supported Pd-Lewis acid catalyst in sc-CO$_2$, while the conditions is so sophisticated (supercritical carbon dioxide as solvent, which requires high H$_2$ and CO$_2$ pressures >7.0 MPa). Most recently, Wang and co-works designed a kind of carbon nitride material as support to prepare Pd-based catalysts[18], which achieved both excellent conversion and selectivity in the hydrogenation of phenol in aqueous media. Nevertheless, the

Key Laboratory of Green Catalysis and Chemical Reaction Engineering of Hunan Province, School of Chemical Engineering Xiangtan University, Xiangtan, 411105, Hunan Province, China. Correspondence and requests for materials should be addressed to J.Z. (email: zhoujicheng@sohu.com)

1

preparation of the mpg-C$_3$N$_4$ and/or CN-x was complicated and involved the use of NH$_4$HF$_2$ or HF which are hazardous. On the other hand, Chen and co-works utilized polymer-fuctionalized CNF and/or ionic liquid-like copolymer to stabilize Pd[19–21], and the as-prepared catalysts have been proven to be efficient for phenol hydrogenation. However, the preparation of these catalysts required many expensive polymers and had the disadvantage of high preparation cost. In this regard, a high efficient selective phenol hydrogenation over on facile catalysts is quiet desirable.

It is generally accepted that the nature of the catalysts support has a considerable impact on the product composition. Scirè *et al.*[22] compared the catalytic performance of Pd/La$_2$O$_3$, Pd/CeO$_2$ and Pd/Al$_2$O$_3$ for phenol hydrogenation, and they found that the order of active and selectivity to cyclohexanone was the following: Pd/La$_2$O$_3$ >Pd/CeO$_2$ >Pd/Al$_2$O$_3$, which is reverse with the order of acidity, in terms of strength and number of acid sites. Corma *et al.*[23] studied the effect of acid-base properties of supports on the phenol hydrogenation. They found that phenol tended to absorb on the basic support, such as MgO, through the hydroxyl group which gave more cyclohexanone. When the support was acidic, such as Al$_2$O$_3$, phenol tended to absorb on the support through aromatic ring and would get more cyclohexanol. Therefore, controlled the nature of support is the key issue to design the Pd-cased for phenol hydrogenation.

Many industrial catalysts consist of expensive metals dispersed on inexpensive high-area porous supports. The high cost of noble metals has limited their industrial applications, and the utilization efficiency of noble metals in conventional supported catalysts is far less than satisfactory. Research has been reported that when the dispersions are high, many of the metal atoms are present at a surface, accessible to reactants and available for catalysis. Flytzani-Stephanopoulos *et al.*[24–26] showed that atomically dispersed Au or Pt cations exhibited excellent catalytic activity for water-gas shift reaction, while Au or Pt particles had no chemical action. Another solution of the significantly reducing the use of precious metal, preparation of support single-atom catalysts (SAC), was proposed by Zhang and coworkers[27–29]. Our group came up with a better strategy to utilize noble metal efficiently, and prepared a novel complex nanostructured catalyst by photocatalytic reduction method[30–32]. Gold nanoparticles were finely dispersed on the nano-TiO$_2$ films, which was tiled on the mesoporous materials MCM-41 or MCM-22. The as-prepared catalysts exhibits fantastic activity and chemical stability for cyclohexane oxidation.

Herein, we present a novel semiconductor nano-film layer supported Pd nanoparticles complex nanostructured catalyst Pd/®-MeO$_x$/AC for high efficient selective hydrogenation of phenol to cyclohexanone. The complex nanostructured catalyst was prepared by a facile method: nano-semiconductor (TiO$_2$ or CeO$_2$) film layer was spread on the high specific surface support (AC) and then Pd nanoparticles were anchored on the nano-semicondutor film layer/AC by photocatalytic reduction method. Furthermore, it is demonstrated that the highly efficient catalytic behavior of Pd/®-TiO$_2$/AC toward phenol selective hydrogenation could be attributed to the synergistic effect between Pd nanoparticles and nano-semiconductor (TiO$_2$ or CeO$_2$) and their complex nanostructured properties.

Results and Discussion

The textural of the samples were investigated by using N$_2$ adsorption-desorption measurements (Figure S1). It is suggested that all the samples is mesoporous following a type IV adsorption isotherm with an important hysteresis loop. Table S1 exhibits the surface area and pore parameters of the prepared catalyst samples. It is noted that the BET surface area of TiO$_2$/AC decreased slightly after loading with Pd nanoparticles, but still had a considerable value of 1138 m^2/g.

The formation of Pd nanoparticles was proven by powder XRD (Fig. 1a). All samples present broadened peaks at 22.6° and 43.3°, which could be attributed to the AC support. It can be observed that 10%®-TiO$_2$/AC and 1–3%Pd/10%®-TiO$_2$/AC exhibit several diffraction peaks at 25.3°, 37.8°, 48.0°, 53.9°, 55.1°, 62.7°, 68.8°, 70.3°, 75.0°, corresponding to (101), (004), (200), (105), (211), (204), (116), (220), and (215) planes of anatase phase of TiO$_2$ (JCPDS 21–1272)[33]. Two addition diffraction peaks at 40.1° and 46.7° could be assigned to the (111) and (200) planes of Pd metal particles in the samples of Pd/10%®-TiO$_2$/AC[34]. It is clear to see that the (111) plane of Pd gets sharper, as the Pd content increased.

Figure 1b shows the FT-IR spectra of the AC, 10%®-TiO$_2$/AC and 2%Pd/10%®-TiO$_2$/AC samples, which presents the vibrations of the various groups at different wavenumbers. For all three samples, a broad peak at 3440 cm^{-1} can be assigned to the stretching vibration of surface-bound O-H groups. A new band at around 1060 cm^{-1} is observable in 10%®-TiO$_2$/AC and 2%Pd/10%®-TiO$_2$/AC, which can be ascribed to Ti-O-C, indicating probably the presence of the interaction between TiO$_2$ and AC[35]. Also, the Ti-O-C band gets stronger in 2%Pd/10%®-TiO$_2$/AC. In addition, AC spectra show two peaks in the region from 1600 to 1700 cm^{-1} identified to C=O group. The region shows a clear red shift when Pd nanoparticles are anchored on the 10%®-TiO$_2$/AC. These changes in FT-IR spectra seem to suggest that an interaction between Pd nanoparticles and ®-TiO$_2$/AC have formed. According to Loh's report[36], a coordination between Pd:O might have formed, that is, the electron pair of O occupy the vacant orbital of Pd. The formed interaction could be an important reason for the high efficient phenol hydrogenation in the presence of Pd/®-TiO$_2$/AC catalyst.

Figure 1c and d display the X-ray photoelectronic profiles of survey and Pd 3d spectra of the 2%Pd/10%®-TiO$_2$/AC catalyst, respectively. As known in Fig. 1d, the Pd presents a doublet corresponding to Pd 3d$_{5/2}$ and Pd 3d$_{3/2}$. The Pd 3d$_{3/2}$ peak at 340.8 eV and the Pd 3d$_{5/2}$ peak at 335.6 eV are attributed to Pd^0, while the peaks at 337.5 eV (Pd 3d$_{3/2}$) and 342.5 eV (Pd 3d$_{5/2}$) can be assigned to Pd^{+2}.

HRTEM micrographs of 10%®-TiO$_2$/AC and 2%Pd/10%®-TiO$_2$/AC are shown in Fig. 2. Proper lattice spacing of the (101) growth direction of anatase TiO$_2$ and the (111) growth direction of Pd nanoparticles are clearly seen in the HRTEM micrographs, which are corroborating the XRD results. The selected area electron diffraction (SAED) patterns of the samples are shown in the insets of the HRTEM images. These images indicate characteristic circles origination from the corresponding crystal planes of anatase TiO$_2$ and Pd nanoparticles. It is noteworthy that only nano TiO$_2$ can be observed in the HRTEM image of 10%®-TiO$_2$/AC, which indicated that
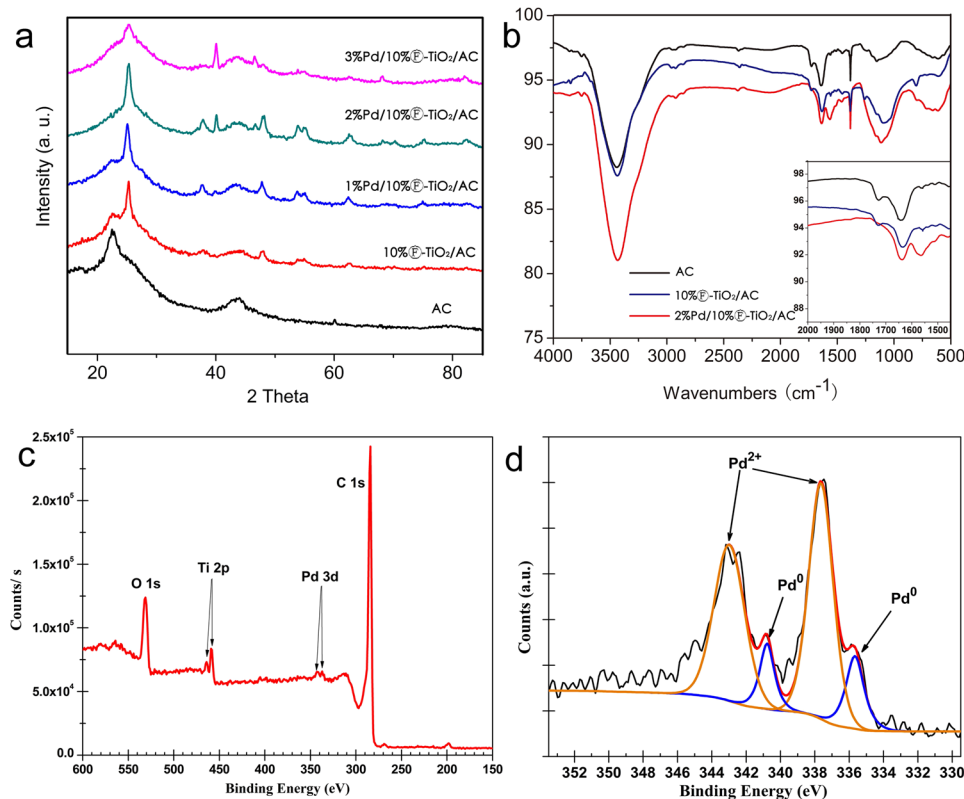
Figure 1. (**a**) XRD patterns of the prepared AC, 10% Ⓟ-TiO$_2$/AC, and 1–3%Pd/Ⓟ-TiO$_2$/AC. (**b**) FT-IR spectra of AC, 10%ⓅTiO$_2$/AC and 2%Pd/10%Ⓟ-TiO$_2$/AC. (**c**) XPS scan survey for Pd/Ⓟ-TiO$_2$/AC catalyst. (**d**) Pd 3d XPS spectra of Pd/Ⓟ-TiO$_2$/AC catalyst.

nano-TiO$_2$ had coated on the activated carbon surface. Figure 3(c) and (d) show the EDX data of 10%Ⓟ-TiO$_2$/AC and 2%Pd/10%Ⓟ-TiO$_2$/AC. The data indicate the presence of elemental constituents within the as-synthesized samples.

Figure 3 shows the TEM images of the Pd/Ⓟ-TiO$_2$/AC samples. The palladium nanoparticles are evident as small dark spots, while the Ⓟ-TiO$_2$/AC substrate is brighter and larger. It can be seen that the palladium nanoparticles are fairly homogeneously distributed over the surface of the Ⓟ-TiO$_2$/AC. As can be seen in the histograms, an increase in the contents of Pd causes an increase in the particle size of the Pd nanoparticles. According to principles of the spontaneous monolayer distribution, 10%Ⓟ-TiO$_2$/AC could construct a platelike semiconductor film supported on AC, thus the as-prepared catalyst Pd/10%Ⓟ-TiO$_2$/AC could form a complex nanostructured composed of nano-semiconductor film layer and Pd nanoparticles.

H$_2$-TPR experiments were performed to further confirm the Pd nanoparticles and the support as shown in Fig. 4. Two positive peaks at 480 °C and 650 °C in the AC sample could be attributed to the oxygen-containing functional groups like -COOH, -OH,=O, etc.[37]. The broad peak observed between 350 °C and 450 °C was due to the reduction of TiO$_2$ in the 10%Ⓟ-TiO$_2$/AC sample. The reduction of Ti^{4+} to Ti^{3+} at relatively low reduction temperature (200 °C) in the presence of Pd. The dissociatively chemisorbed hydrogen on palladium may diffuse from Pd surface to TiO$_2$ and reduce Ti^{4+} to Ti^{3+} [38].

The activity of Pd/Ⓟ-TiO$_2$/AC catalyst for phenol hydrogenation was investigated. Corresponding results are listed in Table 1. The support Ⓟ-TiO$_2$/AC showed no activity (Table 1, entry 1), whereas remarkable conversion and selectivity could be achieved with Pd loading on Ⓟ-TiO$_2$/AC at 70 °C. When TiO$_2$ loading was lower (Table 1, entry 2 and 3), phenol could not convert fully. When TiO$_2$ loading was higher (Table 1, entry 4 and 5), the reaction stayed a conversion of exceeding 99.9 but slightly reduced the selectivity to cyclohexanone. With a fixed mole ratio of Pd and phenol, the conversion and selectivity remained about at the same, regardless of the loading of Pd (Table 1, entry 4, 6 and 7). The reaction was accelerated at higher temperature (Table 1, entry 6, 8–10). A fully conversion with a stable selectivity (around 97%) could be obtained in 1.5 h at 85 °C. It's interesting that increasing the mole ratio of Pd and phenol could also accelerate the reaction (Table 1, entry 11 and 12). Notably, the mole ratio (0.5%) of Pd and phenol used here was rather lower than those in previous reports[17–21], that is, the Pd/Ⓟ-TiO$_2$/AC showed a higher efficiency than those reported catalysts to convert the same amount of phenol. The as-prepared complex nanostructured provide high dispersion and more contact interface with Pd nanoparticles. Thus, the outstanding performance of the as-prepared catalyst Pd/Ⓟ-TiO$_2$/AC could be ascribed to the synergistic effect of metal nanoparticles and nano-semiconductor film layer, and the enhanced effect of electronic and the excellent charge transfer.
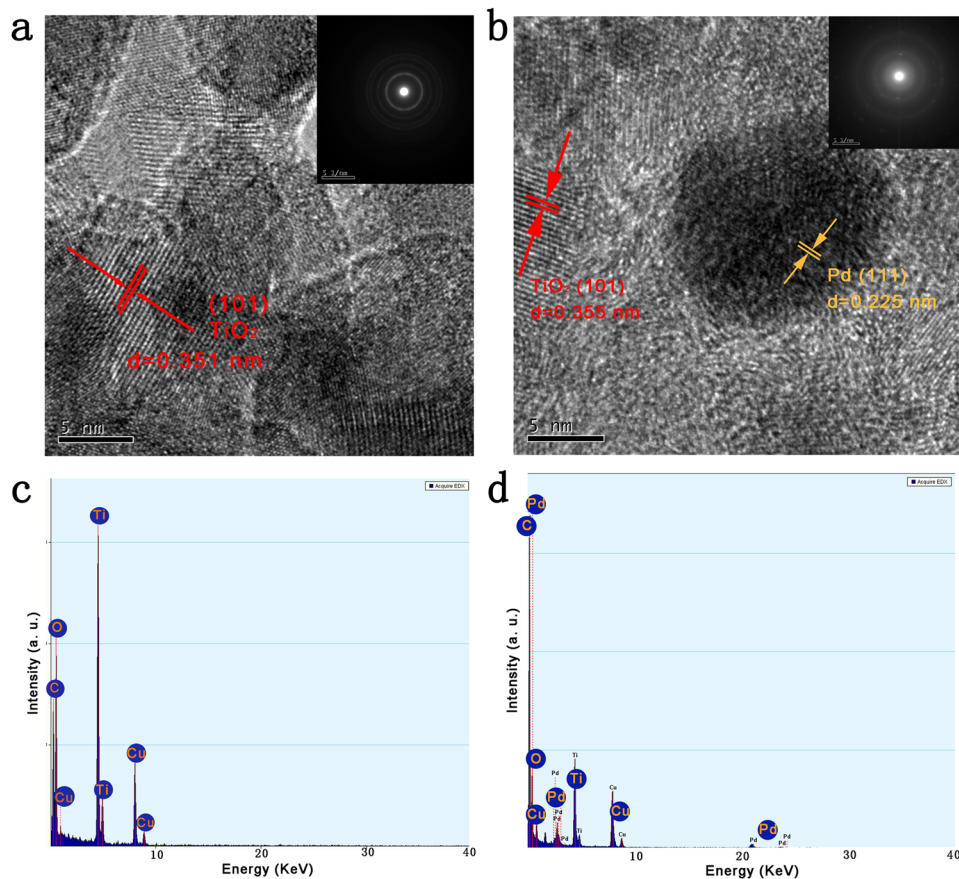
Figure 2. (**a**) HRTEM image of 10%Ⓕ-TiO$_2$/AC. (**b**) HRTEM image of 2%Pd/10%Ⓕ-TiO$_2$/AC. The insets of (**a** and **b**) are the corresponding SAEM images. (**c** and **d**) are EDX analysis of 10%Ⓕ-TiO$_2$/AC and 2%Pd/10%Ⓕ-TiO$_2$/AC, respectively.
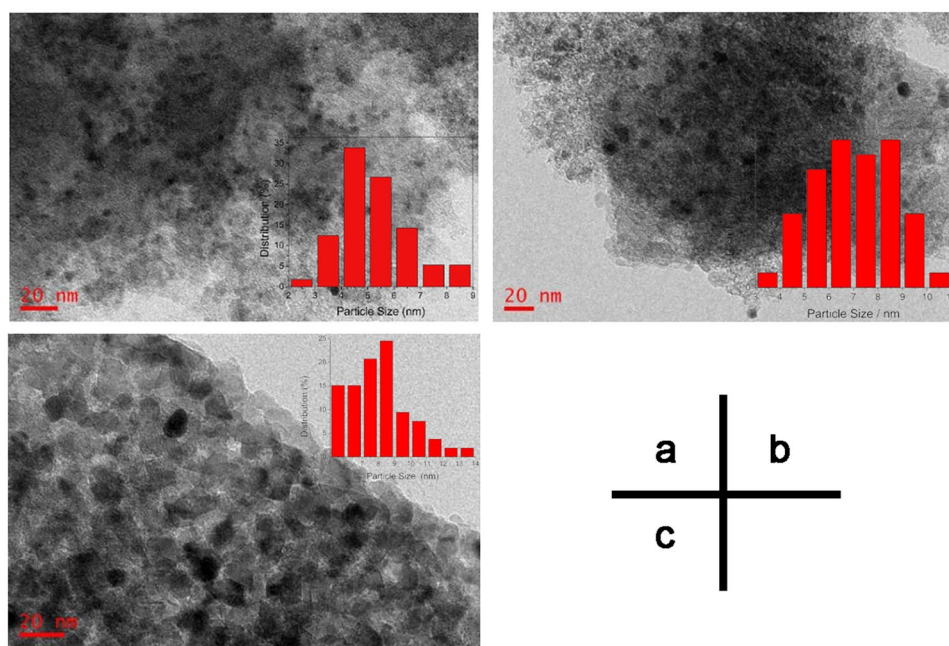
Figure 3. TEM images and Pd nanoparticles size distributions of 1%Pd/10%Ⓕ-TiO$_2$/AC (**a**), 2%Pd/10%Ⓕ-TiO$_2$/AC (**b**), 3%Pd/10%Ⓕ-TiO$_2$/AC (**c**).
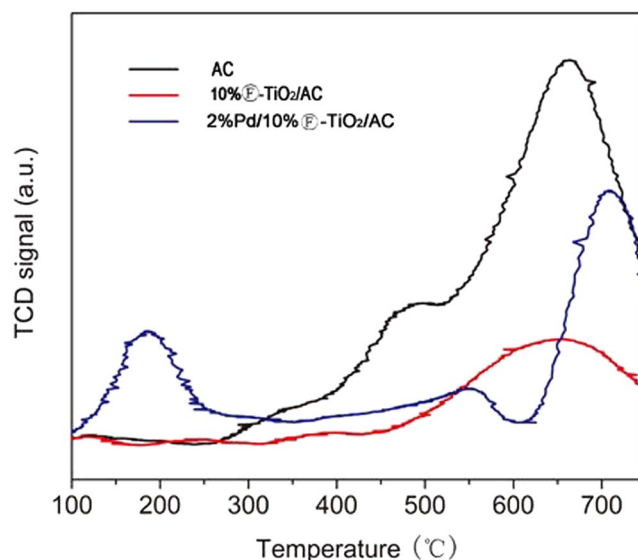
Figure 4. The H$_2$-TPR profiles of AC, 10%℗-TiO$_2$/AC and 2%Pd/10%℗-TiO$_2$/AC.

Entry	Pd (wt. %)	TiO$_2$ (wt.%)	T (°C)	Times (h)	Conversion (%)	Selectivity[b] (%) C=O	OH
1	0	10	70	5	—	—	—
2	2	0	70	2	66.6	96.0	4.0
3	1	5	70	2	86.9	97.1	2.9
4	1	10	70	2	>99.9	97.5	2.5
5	1	15	70	2	>99.9	96.7	3.3
6	2	10	70	2	>99.9	97.1	2.9
7	3	10	70	2	>99.9	96.7	3.3
8	2	10	40	10	>99.9	96.5	3.5
9	2	10	55	5	>99.9	96.7	3.3
10	2	10	85	1.5	>99.9	96.9	3.1
11[c]	2	10	70	0.5	93.0	98.6	1.4
12[d]	2	10	70	1	>99.9	97.8	2.2
13[e]	2	10	70	2	2.1	—	—

Table 1. Hydrogenation of phenol with Pd/℗-TiO$_2$/AC catalyst under various conditions[a]. [a]Reaction conditions: phenol (0.353 g, 3.75 mmol), Pd (0.5 mol% relative to phenol), ichlomethane (20 mL), PH_2 (5 bar), unless otherwise noted. [b]C=O indicates cyclohexanone and C–OH indicates cyclohexanol. [c]n_{Pd}: n_{phenol} = 1.5%; [d]n_{Pd} :n_{phenol} = 1%; [e]substrate: cyclohexanone (0.368 g, 3.75 mmol).

To further understand the high selectivity, we used cyclohexanone as substrate to conduct hydrogenation experiment. The result showed that Pd/℗-TiO$_2$/AC exhibited poor catalytic activity (Table 1, entry 13). Thus, the high hydrogenation selectivity of phenol to cyclohexanone could be attributed to the inhibition of cyclohexanone further hydrogenation to cyclohexanol by Pd/℗-TiO$_2$/AC.

Generally, it is believed that the phenol hydrogenation proceeds under the cooperation between two types of activation work[22, 39]. One is the chemisorbed of phenol on the support, and the other is the activation of H$_2$ on the adjacent Pd species. The adsorption orientation of phenol contains two modes: co-planar and non-planar. The former is formed by the aromatic ring connecting with the support surface, which tends to end up with the complete hydrogenation to cyclohexanol. The latter is formed by the oxygen atom linking with the support surface, which is favor of partial hydrogenation to cyclohexanone. Based on these results, we put forward the possible mechanism of phenol hydrogenation on Pd/℗-TiO$_2$/AC (Figure S2). In the first step, most phenol is adsorbed on ℗-TiO$_2$/AC in non-planar orientation, slightly in co-planar orientation, because TiO$_2$ is an amphiprotic oxide. Then, the adsorbed phenol is partially hydrogenated to cyclohexene by the activated hydrogen on the adjacent Pd nanoparticles. A co-planar adsorption orientation of cyclohexene could be easily hydrogenated to cyclohexanol because of the stronger chemisorption between the benzene ring and support, while the adsorbed cyclohexene in non-planar adsorption prefers to isomerize to give cyclohexanone quickly and leaves the surface of the catalyst rapidly because of only a weaker H-brige donor between the product and support.

Entry	Pd	CeO$_2$	T(°C)	t(h)	Conversion (%)	Selectivity[b] (%) C=O	-OH
1	2	5	70	2	77.5	97.3	2.7
2	2	10	70	1.5	99.8	97.3	2.7
3	2	15	45	3	71.1	97.5	2.5
4	2	15	60	2.5	97.0	99.6	0.4
5	2	15	70	2	>99.9	95.6	4.4
6	2	15	80	1	>99.9	97.7	2.3

Table 2. Hydrogenation of phenol with Pd/Ⓔ-CeO$_2$/AC catalyst under various conditions[a]. [a]Reaction conditions: phenol (0.353 g, 3.75 mmol), Pd (0.5 mol % relative to phenol), dichlomethane (20 mL), PH_2 (5 bar), unless otherwise noted. [b]C=O indicates cyclohexanone and C-OH indicates cyclohexanol.

Entry	catalyst	n$_{Pd}$:n$_{phenol}$ (%)	T (°C)	time (h)	conv. (%)	sel. (%) C=O	C-OH	TOFs (h^{-1})[a]	Refs
1	Pd/Ⓔ-TiO$_2$/AC	0.5	70	2	>99.9	97.5	2.5	100	This work
2	Pd/Ⓔ-CeO$_2$/AC	0.5	80	1	>99.9	97.7	2.3	200	This work
3	Pd/C-AlCl$_3$	5	80	3	>99.9	99.3	0.7	6.67	17
4	Pd-mpg-C$_3$N$_4$	5	65	2	>99.9	>99	<1	10	18
5	Pd-PANI/CNT	5	80	9	>99.9	>99	<1	2.22	19
6	Pd-HPW	5	80	7	>99	>99	<1	2.86	21
7	PdAu/MHSS	2.5	50	0.75	97.5	96.6	3.4	52	15

Table 3. Comparison of different catalysts for phenol hydrogenation. [a]TOFs = mole of product/(moles of Pd * reaction times).

Moreover, the electron-rich Pd nanopaticles could activate more H$_2$ molecules. AC with abundant oxygen-containing group provide not only many electron, but also highly specific areas for the nanostructured of Pd and TiO$_2$, which benefit mass transfer and the contact of reactants with active sites in phenol hydrogenation.

To further understand the synergistic effect of metal nanoparticles and nano-semiconductor film layer, we investigate the phenol hydrogenation over Pd/Ⓔ-CeO$_2$/AC catalysts. (Table 2). As can be seen, the reaction reached completion in 1 hour and the selectivity attained >97% at 80 °C when 2%Pd/15%Ⓔ-CeO$_2$/AC was used as catalyst (Table 2, entry 6). Interestingly, the conversion of phenol was low (77.5%) when the loading of CeO$_2$ was 5%, while the conversion reached to >99% when CeO$_2$ content was 10% or 15%. We believe these could be attribute to the nano-Ⓔ-CeO$_2$ layer have not formed when the CeO$_2$ loading was low so that the complex nano-structured of Pd/Ⓔ-CeO$_2$ had not formed completely. Similar to Pd/Ⓔ-TiO$_2$/AC, the phenol hydrogenation was accelerated at higher temperature over Pd/Ⓔ-CeO$_2$/AC catalyst.

To unveil the underlying factors that provide the superior activity of the hydrogenation over Pd/Ⓔ-MeO$_x$/AC catalysts, we compared the TOFs for the hydrogenation of phenol over Pd/Ⓔ-MeO$_x$/AC and other catalytic systems. As shown in Table 3, the results showed that Pd/Ⓔ-MeO$_x$/AC catalysts gave a TOF of 200 h^{-1}, an order of magnitude higher than traditional catalysts and 3.8-fold higher than that of the best reported catalyst PdAu/MHSS (ref. 15). It illustrated that the combination of nano-metal and nano-semiconductor, which both possess redox catalytic mechanism, was an efficient catalytic system and exhibited outstanding activity and selectivity for phenol hydrogenation.

To fully illustrate the superiority catalytic performance of the complex nanostructured catalysts, we compared the catalytic results of the as-prepared Pd/Ⓔ-MeO$_x$/AC, Pd/MeO$_x$ and Pd/AC. As summarized in Table 4, Pd nan-oparticles supported on the AC without metal oxide showed moderate activity for phenol hydrogenation (Table 4, entry 3). When Pd nanoparticles were supported on MeO$_x$ (TiO$_2$ or CeO$_2$) simply without AC, the as-prepared samples had poor activity for phenol hydrogenation (Table 4, entries 4–5). Wang's work[31] also illustrated the poor hydrogenation over Pd/MeO$_x$ catalysts (Table 4, entries 6–7). Nevertheless, catalysts Pd/Ⓔ-MeO$_x$/AC, which were equipped with complex nanostructured of nano-Pd and nano-semiconductors film layer supported on the large surface support, exhibited predominant catalytic performance for phenol hydrogenation. In comparison with Pd/MeO$_x$ catalysts, we could generalize two major structure features of the as-prepared Pd/Ⓔ-MeO$_x$/AC: nano-metal and nano-semiconductor film layer supported on the large surface support and greatly increasing of contact interface of nano-metal-semiconductors. Owing to these excellent features, the properties of Pd/Ⓔ-MeO$_x$/AC got improved: the synergistic effect of metal nanoparticles and nano-semiconductors support layer, the enhanced effect of electronic and the excellent charge transfer, and all these improvements may contribute to the enhanced catalytic performance.

Conclusion

In summary, a novel catalyst Pd/Ⓔ-MeO$_x$/AC with complex nanostructured has been prepared by the photocat-alytic reduction method. Palladium nanoparticles have been equably anchored on the nano-ⒺTiO$_2$ film layer,

Entry	Catalysts	T(°C)	t(h)	Conversion (%)	Selectivity[a] (%)		
					C=O	C-OH	Reference
1[b]	Pd/℗-TiO2/AC	70	2	>99.9	97.1	2.9	This work
2[b]	Pd/℗-CeO$_2$/AC	70	1.5	99.8	97.3	2.7	This work
3[b]	Pd/AC	70	2	66.6	96.0	4.0	This work
4[b]	Pd/TiO$_2$	70	2	6.4	99.4	0.6	This work
5[b]	Pd/CeO$_2$	70	2	3.4	99.2	0.8	This work
6[c]	Pd/TiO$_2$	65	6	8	99	1	40
7[c]	Pd/CeO$_2$	65	6	2	100	0	40

Table 4. Catalytic results for Pd/℗-MeO$_x$/AC, Pd/AC and Pd/MeO$_x$ catalysts. [a]C=O indicates cyclohexanone and C-OH indicates cyclohexanol. [b]Reaction conditions: phenol (0.353 g, 3.75 mmol), Pd (0.5 mol % relative to phenol), dichlomethane (20 mL), P$_{H2}$ (5 bar). [c]Reaction conditions: phenol 0.585 mmol, Pd (4 mol% relative to phenol), solvent 2 ml H$_2$O, H$_2$ 1 bar, reaction temperature 65 °C.

which was spread on the high specific surface AC. Due to the complex nanostructured of metal nanoparticle and nano-semiconductors support layer, the as-prepared Pd catalyst Pd/℗-MeO$_x$/AC exhibits a high activity for the phenol selective hydrogenation. The hydrogenation proceeds efficiently, with a lower mole ratio of Pd and phenol (0.5%) under the pressure of 0.7 MPa at 70 °C. The synergistic effect of metal nanoparticle and nano-semiconductors support layer, nano-metal-semiconductors heterojunction on the large surface support and greatly increasing of contact interface of nano-metal-semiconductors, the enhanced effect of electronic and the excellent charge transfer all could attribute to the outstanding catalytic performance. This work open a promising avenue for developing new supported metal catalyst with complex nanostructured of nano-Pd (Au, Pt, Rh, Ag, Ni, *et al.* metals) and nano-semiconductors film layer supported on the large surface support for efficient hydrogenation and redox reaction.

Methods
Synthesis. *Pretreatment of activated carbon with acid.* A commercial activated carbon (AC) made from coconut shells (Fujian Xinsen Carbon Co. Ltd.) was washed and boiled for 2–3 times. The activated carbon was pretreated with HNO$_3$ (10%) at 60 °C under refluxing for 2 h, and eventually washed to neutrality with distilled water. Then the sample was dried at 80 °C for 12 h.

Preparation of ℗-TiO$_2$/AC support. The activated carbon was modified with 5, 10, 15 wt.% ℗-TiO$_2$ by sol-gel. Typically, 3 g tetra-n-butyl titanate was first dissolved in 25 mL ethanol by stirring and then 1.3 mL acetic acid was added into the mixture to obtain solution A. A solution of 15 mL ethanol and 1.5 mL distilled water was denoted by solution B. Then solution B was added into solution A dropwise under vigorous stirring to form sol C. Subsequently, the pretreatment AC was dispersed into sol C and nitric acid was used to adjust pH to 3. After being treated by ultrasonic agitation, the mixture was left at ambient temperature to form gel. The obtained material was dried at 80 °C for 12 h, and then calcined at 550 °C for 2 h. According to the principles of the spontaneous monolayer distribution, TiO$_2$ loaded on the AC with monolayer or multilayers, rather than stacking pattern, by adjusting the loading of TiO$_2$. The content of TiO$_2$ was measured by ICP-AES analysis (Table S2). The as-prepared material was denoted as 10%℗-TiO$_2$/AC.

Preparation of Pd-supported catalyst by the photocatalytic reduction method. The as-prepared TiO$_2$/AC support (0.586 g) was dispersed in 100 mL distilled water and 3 mL methanol. Then the mixture was treated by ultrasonic agitation for 30 min. 1 mL of H$_2$PdCl$_4$ aqueous solution (0.0119 g/mL) was added into the slurry under stirring. The suspension was irradiated with a 15 W UV lamp for 10 h which is sufficient for deposition of palladium at ambient temperature. Finally, the sample was separated by filtration, washed several times by distilled water up to pH 7, dried in a vacuum oven for 10 h. This sample will be referred as Pd/℗-TiO$_2$/AC. The load of Pd was measured by ICP-AES analysis and the results showed that the loading efficiency of Pd exceeded 98% (Table S2). Here, we use the theory content of Pd to describe the as-prepared catalysts. The principle of photocatalytic reduction method could been summarized as following:

$$TiO_2 + hv \rightarrow TiO_2(e^- + h^+) \tag{1}$$

$$Pd^{2+} + 2e^- \rightarrow Pd \tag{2}$$

$$O_2 + 4H^+ + 4e^- \rightarrow 2H_2O \tag{3}$$

$$2H_2O + 4h^+ \rightarrow O_2 + 4H^+ \tag{4}$$

$$\text{Total reaction: } 2Pd^{2+} + 2H_2O \xrightarrow{hv} 2Pd + O_2 + 4H^+ \tag{5}$$
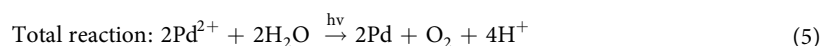
Phenol Hydrogenation. Hydrogenation of phenol was performed in a 50 mL Teflon-lined stainless steel autoclave. Typically, 0.353 g phenol, a given amount of Pd catalyst (Pd/phenol = 0.005, 0.01, 0.015 (ratio of mole)) and 20 mL dichloromethane were loaded into the reactor. The autoclave was sealed and purged three times with H_2 to remove the air. Then the reactor was placed in an oil bath. Hydrogen was introduced into the reactor after desired temperature was reached and the stirrer was started. After the reaction, the reactor was cooled to room temperature and the products were analyzed on GC (Figure S3).

The conversion and selectivity are defined as follows:

$$\text{Conversion of phenol (\%)} = \frac{\text{Moles of phenol converted}}{\text{Moles of phenol initially added}} * 100\% \tag{6}$$

$$\text{Selectivity to cyclohexanone (\%)} = \frac{\text{Moles of cyclohexanone}}{\text{Moles of phenol converted}} * 100\% \tag{7}$$

Characterization. X-ray diffraction (XRD) of samples was obtained on a Rigaku D/max-II/2500 X-ray powder diffractometer, Cu Ka radiation was employed and the working voltage and current were 40 kV and 30 mA, respectively. Surface images of the samples were investigated by a JEM2010 transmission electron microscopy (TEM). High resolution transmission electron microscopy (HRTEM) images were obtained using a JEOL JEM-2100F transmission electron microscope at an acceleration voltage of 200 kV. Fourier transform infrared (FT-IR) spectra were recorded by using a Nicolet 380 spectrometer from 4000 to 400 cm^{-1}, and the KBr pellet technique was used. X-ray photoelectron spectroscopy (XPS) was performing using ESCALAB 250Xi (Thermo) with Al Kα radiation. Inductively coupled plasma-atomic emission spectrometry (ICP-AES) data were obtained using an Intrepid II XSP (IRIS). H_2 temperature programmed reduction (H_2-TPR) were carried out on ChemBET 3000 with a thermal conductivity detector. The samples were treated at 250 °C for 1 h under Ar atmosphere, then cooled down to 80 °C. After pre-treated, temperature was increased to 700 °C at the heating rate of 10 °C/min in a 10% H_2/Ar stream.

References

1. Weissermel, K. & Arpe, H. J. Industrial Organic Chemistry. Wiley-VHC, Weinheim (1997).
2. Jhansi, M., Kishore, L., Anand, K. A. & Kumar, A. Kinetic study of oxidation of cyclohexanol using bimetallic iron-copper macrocyclic complex catalyst. *Catal. Commun.* **10**, 285–290 (2008).
3. Mahata, N., Raghavan, K. V., Vishwanathan, V. & Keane, M. A. Influence of the charge transfer capacity of alkali and alkaline earth metals as promoters in thehydrogenation of phenol over palladium and nickel catalysts. *React. Kinet. Catal. Lett.* **72**, 297–302 (2001).
4. Scirè, S., Crisafulli, C., Maggiore, R., Minicò, S. & Galvagno, S. FT-IR characterization of alkali-doped Pd catalysts for the selective hydrogenation of phenol to cyclohexanone. *Appl. Surf. Sci.* **93**, 309–316 (1996).
5. Neri, G. *et al*. Hydrogenation of phenol to cyclohexanone over palladium and alkali-doped palladium catalysts. *Appl. Catal. A Gen.* **110**, 49–59 (1994).
6. Claus, P. *et al*. Pd/MgO Catalyst characterization and phenol hydrogenation activity. *J. Catal.* **192**, 88–97 (2000).
7. Shore, S. G., Ding, E. R., Park, C. & Keane, M. A. Vapor phase hydrogenation of phenol over silica supported Pd and Pd-Yb catalysts. *Catal. Commun.* **3**, 77–84 (2002).
8. Narayanan, S. & Krishna, K. Structure activity relationship in Pd/hydrotalcite: effect of calcination of hydrotalcite on palladium dispersion and phenol hydrogenation. *Catal. Today* **49**, 57–63 (1999).
9. Mahata, N. & Vishwanathan, V. Influence of palladium precursors on structural properties and phenol hydrogenation characteristics of supported palladium catalysts. *J. Catal.* **196**, 262–270 (2000).
10. Xiang, Y. Z. *et al*. Reaction performance of hydrogen from aqueous-phase reforming of methanol or ethanol in hydrogenation of phenol. *Ind. Eng. Chem. Res.* **50**, 3139–3144 (2011).
11. Makowski, P., Cakan, R. D., Antonietti, M., Goettmann, F. & Titirici, M. M. Selective partial hydrogenation of hydroxy aromatic derivatives with palladium particle supported on hydrophillic carbon. *Chem. Commun.* **8**, 999–1001 (2008).
12. Díaz, E., Mohedano, A. F., Calvo, L., Gilarranz, M. A. & Rodríguez, J. J. Hydrogenation of phenol in aqueous phase with palladium on activated carbon catalysts. *Chem. Eng. J.* **131**, 65–71 (2007).
13. Chatterjee, M. *et al*. Hydrogenation of phenol in supercritical carbon dioxide catalyzed by palladium supported on Al-MCM-41: a facile route for one-pot cyclohexanone formation. *Adv. Synth. Catal.* **351**, 1912–1924 (2009).
14. Yang, X., Liao, S., Zeng, J. & Liang, Z. A mesoporous hollow silica sphere (MHSS): Synthesis through a facile emulsion approach and application of support for high performance Pd/MHSS catalyst for phenol hydrogenation. *Appl. Sur. Sci.* **257**, 4472–4477 (2011).
15. Yang, X., Du, L., Liao, S. J., Li, Y. X. & Song, H. Y. High-performance gold-promoted palladium catalyst towards the hydrogenation of phenol with mesoporous hollow spheres as support. *Catal. Commun.* **17**, 29–33 (2012).
16. Liu, H. L., Li, Y. W., Luque, R. & Jiang, H. F. A tuneable bifunctional water-compatible heterogeneous catalyst for the selective aqueous hydrogenation of phenols. *Adv. Synth. Catal.* **353**, 3107–3113 (2011).
17. Liu, H., Jiang, T., Han, B., Liang, S. & Zhou, Y. Selective phenol hydrogenation to cyclohexanone over a dual supported Pd-lewis acid catalyst. *Science* **326**, 1250–1252 (2009).
18. Wang, Y., Yao, J., Li, H. R., Su, D. S. & Antonietti, M. Highly selective hydrogenation of phenol and derivatives over a Pd-carbon nitride catalyst in aqueous media. *J. Am. Chem. Soc.* **133**, 2362–2365 (2011).
19. Chen, J. Z. *et al*. Direct selective hydrogenation of phenol and derivatives over polyaniline-functionalized carbon-nanotube-supported palladium. *ChemPlusChem* **78**, 142–148 (2013).
20. Chen, A. B. *et al*. Selective hydrogenation of phenol and derivatives over polymer-functionalized carbon-nanofiber-supported palladium using sodium formate as the hydrogen source. *ChemPlusChem* **78**, 1370–1378 (2013).
21. Chen, A. B., Zhao, G. Y., Chen, J. Z., Chen, L. M. & Yu, Y. F. Selective hydrogenation of phenol and derivatives over an ionic liquid-like copolymer stabilized palladium catalyst in aqueous media. *RSC Advances* **3**, 4171–4175 (2013).
22. Scirè, S., Minicò, S. & Crisafulli, C. Selective hydrogenation of phenol to cyclohexanone over supported Pd and Pd-Ca catalysts: an investigation on the influence of different supports and Pd precursors. *Appl. Catal. A Gen.* **235**, 21–31 (2002).
23. Pérez, Y., Fajardo, M. & Corma, A. Highly selective palladium supported catalyst for hydrogenation of phenol in aqueous phase. *Catal. Commun.* **12**, 1071–1074 (2011).
24. Fu, Q., Saltsburg, H. & Flytzani-Stephanopoulos, M. Active nonmetallic Au and Pt species on ceria-based water-gas shift catalysts. *Science* **301**, 935–938 (2003).

25. Qi, F., Deng, W., Saltsburg, H. & Flytzani-Stephanopoulos, M. Activity and stability of low-content gold-cerium oxide catalysts for the water-gas shift reaction. *Appl. Catal. B Environ.* **56**, 57–68 (2005).

26. Ming, Y., Allard, L. F. & Maria, F. S. Atomically dispersed Au-(OH)$_x$ species bound on titania catalyze the low-temperature water-gas shift reaction. *J. Am. Chem. Soc.* **135**, 219–224 (2013).

27. Qiao, B. *et al*. Single-atom catalysis of co oxidation using Pt1/FeO$_x$. *Nat. Chem.* **3**, 634–641 (2011).

28. Lin, J. *et al*. Remarkable performance of Ir1/FeO$_x$ single-atom catalyst in water gas shift reaction. *J. Am. Chem. Soc.* **135**, 15314–15317 (2013).

29. Yang, X. F. *et al*. Single-atom catalysts: a new frontier in heterogeneous catalysis. *Accounts Chem. Res.* **46**, 1740–8 (2013).

30. Zhou, J. C., Yang, X. F., Wang, Y. Q. & Chen, W. J. An efficient oxidation of cyclohexane over Au@TiO2/MCM-41 catalyst prepared by photocatalytic reduction method using molecular oxygen as oxidant. *Catal. Commum.* **46**, 228–233 (2014).

31. Li, L., Zhou, J. C., Xie, Z. B. & Ouyang, W. B. Preparation of Au nanoparticles its catalytic performance for catalyst Au@TiO2/MCM-22 and cyclohexane selective oxidation. *Acta Petrolei Sinica* **29**, 975–983 (2013).

32. Wang, Y. Q., Zhou, J. C. & Yang, X. F. Preparation of nano-sized gold-doped TiO$_2$ catalyst and its performance for selective oxidation of cyclohexane at low temperature. Chin. *J. Process Eng.* **6**, 1186–1191 (2009).

33. Liu, X. J., Pan, L. K., Lv, T., Sun, Z. & Sun, C. Q. Sol-gel synthesis of Au/N-TiO$_2$ composite for photocatalytic reduction of Cr(VI). *RSC. Adv.* **2**, 3823–3827 (2012).

34. He, F., Liu, J. C., Roberts, C. B. & Zhao, D. Y. One-step "green" synthesis of Pd nanoparticles of controlled size and their catalytic activity for trichloroethene hydrodechlorination. *Ind. Eng. Chem. Res.* **48**, 6550–6557 (2009).

35. Liu, S. X., Chen, X. Y. & Chen, X. A TiO2/AC composite photocatalyst with high activity and easy separation prepared by a hydrothermal method. *J. Hazard. Mater.* **143**, 257–263 (2007).

36. Jahan, M., Liu, Z. L. & Loh, K. P. A Graphene Oxide and Copper-Centered Metal Organic Framework Composite as a Tri-Functional Catalyst for HER, OER, and ORR. *Adv. Funct. Mater.* **23**, 5363–5372 (2013).

37. Shekar, S. C., Murthy, J. M., Rao, P. K. & Rao, K. S. R. Selective hydrogenolysis of dichlorodifluoromethane on carbon covered alumina supported palladium catalyst. *J Mol. Catal. A-Chem.* **191**, 45–59 (2003).

38. Xu, J., Sun, K., Zhang, L., Ren, Y. & Xu, X. A highly efficient and selective catalyst for liquid phase hydrogenation of maleic anhydride to butyric acid. *Catal. Commun.* **6**, 462–465 (2005).

39. Cheng, L., Dai, Q. G., Li, H. & Wang, X. Y. Highly selective hydrogenation of phenol and derivatives over Pd catalysts supported on SiO$_2$ and Y-Al$_2$O$_3$ in aqueous media. *Catal. Commun.* **57**, 23–28 (2014).

40. Li, Y. *et al*. Highly Selective Pd@mpg-C$_3$N$_4$ catalyst for phenol hydrogenation in aqueous phase. *RSC. Adv.* **3**, 10973–10982 (2013).

Author Contributions

J.S. and J.Z. designed the project and wrote the main manuscript text. J.S., W.O. and Y.Z. accomplished the experiment work together. J.S., W.X. and J.Z. made the results analysis. All authors reviewed the manuscript.

Additional Information